JOC The Journal of Organic Chemistry

Article

On the Non-Innocent Behavior of Substrate Backbone Esters in Metal-Catalyzed Carbocyclizations and Friedel-Crafts Reactions of Enynes and Arenynes

Bastien Michelet, Guillaume Thiery, Christophe Bour, and Vincent Gandon

J. Org. Chem., **Just Accepted Manuscript** • DOI: 10.1021/acs.joc.5b02052 • Publication Date (Web): 08 Oct 2015

ACS Publications

The Journal of Organic Chemistry is published by the American Chemical Society.
1155 Sixteenth Street N.W., Washington, DC 20036

On the Non-Innocent Behavior of Substrate Backbone Esters in Metal-Catalyzed Carbocyclizations and Friedel-Crafts Reactions of Enynes and Arenynes

Bastien Michelet,[†] Guillaume Thiery,[†] Christophe Bour,[†] and Vincent Gandon[†,§,*]

[†] *ICMMO (UMR CNRS 8182), Université Paris-Sud, Bâtiment 420, 91405 Orsay cedex, France*

[§] *Institut de Chimie des Substances Naturelles, CNRS, Avenue de la Terrasse, 91198 Gif-sur-Yvette Cedex, France*

vincent.gandon@u-psud.fr

Abstract: On the basis of DFT computations and experimental results, we show that the presence of the ester group in the backbone of organic substrates can influence the mechanism of metal-catalyzed carbocyclization reactions. The non-innocent role of the ester functionality in lowering the activation barrier of the key step of the gallium- and indium-catalyzed cycloisomerization of 1,6-enynes is revealed. In the case of the gallium-catalyzed hydroarylation of arenynes, the esters in the tether can deprotonate the Wheland intermediate, thus avoiding more energetically demanding [1,3]- or [1,2]/[1,2]-H shifts. As for the gallium-catalyzed Friedel-Crafts alkylation, an unusual concerted S_EAr mechanism involving the esters has been calculated. Lastly, computations evidence that the ester group of methyl propiolates enables a divergent mechanism in the platinum-catalyzed intramolecular hydroarylation.

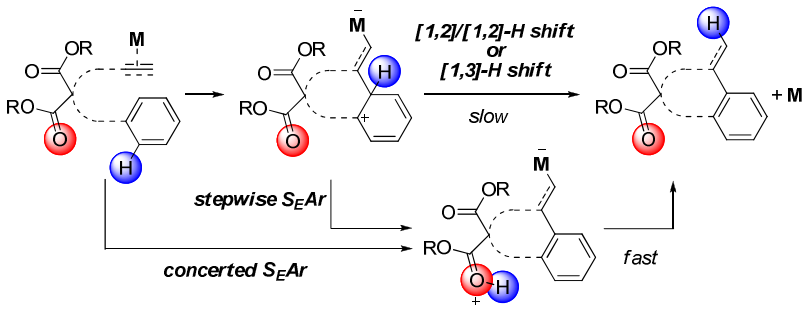

1- Introduction.

The synthesis of polyunsaturated substrates for metal-catalyzed reactions such as cycloisomerizations, metatheses, cycloadditions, etc., typically starts from an active methylene compound which is sequentially functionalized under basic conditions to form enynes, diynes, dienes, arenynes, etc. (Scheme 1). The electron-withdrawing groups of the starting active methylene compound usually remain as part of the tether between the unsaturated C-C bonds and their presence is well-tolerated in most cases.

Scheme 1. Synthesis of Polyunsaturated Precursors from Active Methylene Compounds

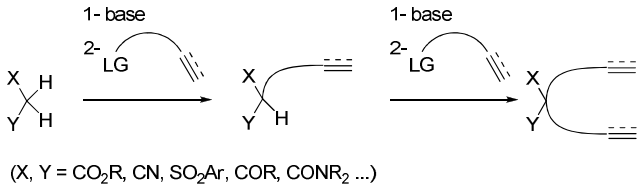

For instance, countless substrates for metal-catalyzed reactions have been straightforwardly constructed by malonic ester synthesis (Chart 1).

Chart 1. Examples of Substrates Used in Metal Catalysis Displaying a *gem*-Diester in the Tether

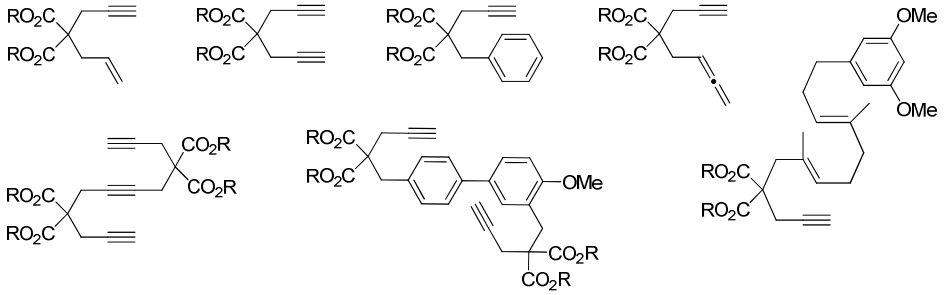

The ease and versatility of this synthetic approach is not its only advantage. It is also well-established that the *gem*-disubstitution of the tether accelerates cyclization steps by Thorpe-Ingold or reactive rotamer effects.[1] One could also envisage that the presence of functional groups in the tether influences the elementary steps of a catalytic cycle in other ways. As they are at the same time electron-withdrawing groups and electron donors though their heteroatom lone pairs, they could possibly exert long range inductive effects, stabilize charges, establish stabilizing non-covalent interactions, capture protons, etc. Some of these aspects are well-known in biology or sugar chemistry for instance, but they have been much less studied in the context of metal-catalyzed reactions. On the basis of DFT calculations, we show in this article that the *gem*-diester in the tether can provide more than a mere kinetic *gem*-disubstituent effect in gallium(III)- and indium(III)-catalyzed C–C bond forming reactions by serving as proton shuttle. In particular, an overlooked base-effect in Friedel-Crafts reactions leading to stepwise or concerted S_EAr pathways is discussed. We finally broaden the discussion to the case of a single ester substituent located at the reactive alkyne unit of a substrate under platinum(II) catalysis, and show that its presence can set up a new mechanistic scenario.

2- Results and Discussion

2.1- Ga(III)- and In(III)-Catalyzed Cycloisomerization of 1,6-Enynes

The metal-catalyzed cycloisomerization of enynes and related compounds is a well-established strategy for the rapid increase of the molecular complexity from simple substrates.[2] While a variety of transition metal complexes can be used as catalysts for this reaction, simple salts derived from polarizable main group elements are also efficient, notably gallium and indium halides.[3] In this section, we briefly reinvestigate part of a previously reported computational study in which the structure of the enynes has been simplified by removing the *gem*-disubstituent in the tethers.

In a series of recent papers, Yu et al used a combined theoretical and experimental approach to identify the real catalytic species in GaX_3- and InX_3-catalyzed cycloisomerization of 1,6-enynes.[4] A large body of their work relies on the reactivity of the *gem*-diester tethered 1,6-enyne **1** which was previously shown by Miyanahana and Chatani to transform into the 1,4-diene **2** (*E*/*Z* mixture)

exclusively in the presence of a catalytic amount of $InCl_3$, and not into the conjugated diene **3** (Scheme 2).[5] Starting from the postulate that almost all catalysts give conjugated dienes with 1,6-enynes except $InCl_3$, Yu et al decided to study this reaction in detail so as to elucidate the origin of this peculiarity. The formation of **2** as a sole product could be reproduced with $GaCl_3$, $GaBr_3$, $InBr_3$, InI_3, as well as with $InCl_3$/AgY mixtures (Y = SbF_6, BF_4, OTf, $OCOCF_3$). The fluorene derivative **4** was also tested and gave rise to the non-conjugated product **5** with $InCl_3$ as catalyst.

Scheme 2. Ga(III)- and In(III)-Catalyzed Cycloisomerization of Enynes 1 and 4

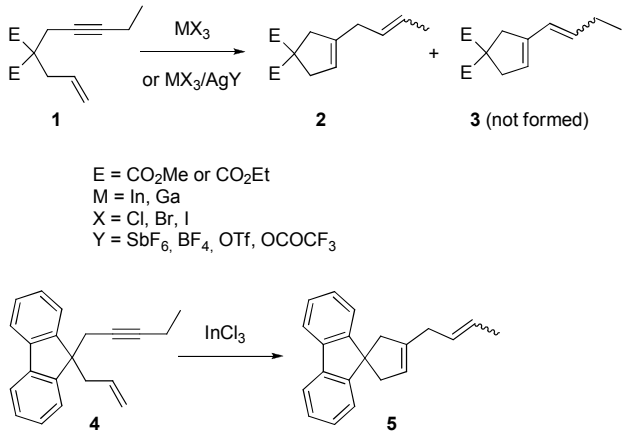

A neutral and a cationic pathway were considered to account for the selective formation of the non-conjugated diene. A simplified overview of the mechanism limited to the most stable *trans*-isomers of **D**, **E**, **H**, and **I** is shown in Scheme 3. In the neutral pathway, enyne **1** forms complex **A** after coordination of MX_3 to the C≡C bond. Nucleophilic attack of the C=C bond provides the non-classical carbocationic species **B** (depicted here as a chosen resonance form instead of the more abstruse resonance hybrid),[3b] which then rearranges into the key intermediate **C**. The latter is the precursor of the isolated product after selective [1,2]-H migration of Hb (see complex **D**). That of Ha on the other hand furnishes the unobserved conjugated product (see complex **E**).

Scheme 3. Possible Mechanistic Pathways of the Ga(III)- and In(III)-Catalyzed Cycloisomerization of Enyne 1

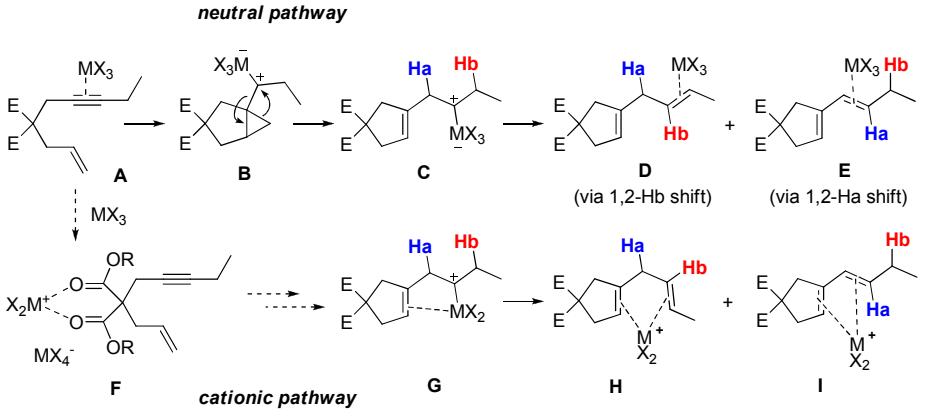

In the papers of Yu et al, calculations were carried out using the B3LYP functional, the LANL2DZ+ECP basis set for In or Ga, the 6-31G(d) basis set for other elements (noted BS1 in Table 1). On the basis of these DFT computations, the neutral pathway was ruled out. For instance, with $GaCl_3$, calculations predict the wrong isomer **E** (see **TSa-GaCl$_3$** vs **TSb-GaCl$_3$** in Table 1, Entry 1).[6] The migration of Ha through **TSa-GaCl$_3$** would require 7.7 kcal/mol of free energy of activation while that of Hb through **TSb-GaCl$_3$** would require 9.7 kcal/mol. We have reproduced these calculations at a slightly different level of theory and reached the same conclusions (Entry 2, B3LYP/6-31G(d) for all atoms (BS2)).

Table 1. Free Energies of Activation (kcal/mol) of the Key Step of the Ga(III)-Catalyzed Cycloisomerization of a Model 1,6-Enyne

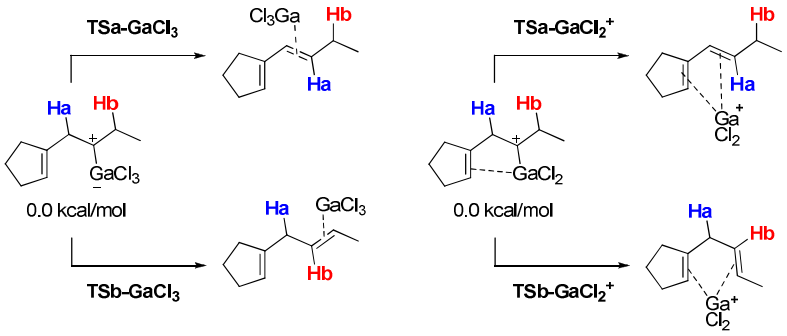

Entry	Theory Level[a]	**TSa-$GaCl_3$**	**TSb-$GaCl_3$**	**TSa-$GaCl_2^+$**	**TSb-$GaCl_2^+$**
1	B3LYP/BS1	7.7	9.7	8.3	5.2
2	B3LYP/BS2	9.1	10.8	6.4	3.0
3	M06-2X/BS3	9.0	9.6	4.4	1.9

[a] BS1: LANL2DZ+ECP (Ga), 6-31G(d) (other elements), values of Entry 1 taken from the Supporting Information of Ref 4c; BS2: 6-31G(d) (all elements); BS3: 6-311+G(d,p) (all elements).

A cationic scenario was then envisaged by Yu et al. They suggested that MX_3 salts could react with the solvent or the substrate to form MX_2^+ ions. An ion peak corresponding to [$InCl_2$+**2**]$^+$ could be detected by ESI-HRMS analysis of a reaction mixture comprising 150 mol% of $InCl_3$, enyne **1**, and acetonitrile. The proposed structure corresponds to **F** in Scheme 3, in which MX_2^+ is coordinated to the ester groups of the tether of the enyne. However, acetonitrile is a solvent in which the reaction cannot occur catalytically.[4a,7] Nevertheless, the possibility that MX_2^+ could be the actual active species was checked computationally by Yu et al. With $GaCl_2^+$ instead of $GaCl_3$, the computations predicted the experimentally observed non-conjugated product as the preferred one (see **TSa-$GaCl_2^+$** vs **TSb-$GaCl_2^+$** in Table 1, Entry 1). Again, we reached the same conclusions with BS2 (Entry 2). It was suggested that the migration of Ha or Hb is encouraged by the electronic effect of the nearby cyclopentene or methyl group. Since the cyclopentene is electron-richer, the migration of Ha should be always favored, as with $GaCl_3$ for instance. Yet, since $GaCl_2^+$ displays two vacant orbitals instead of

one in $GaCl_3$, complexation of the C=C bond in the key intermediate becomes possible. This electron depletion renders the terminal methyl group electron-richer, hence the preferred migration of Hb with $GaCl_2^+$.

Yu et al now recommend the use of 1,6-enynes as mechanistic probes to identify the real active species when GaX_3 or InX_3 salts are used as catalysts.[4c] If the reaction of **1** gives **2**, then the active species should be GaX_2^+ or InX_2^+, and not GaX_3 or InX_3. On the other hand, if the conjugated product **3** is obtained, then only the neutral pathway could explain its formation. Our research group has specialized in the use of neutral and cationic gallium and indium complexes in molecular catalysis.[8] In particular, we have developed the synthesis of complexes of type $[IPr{\cdot}MX_2]^+[Y]^-$ (M = Ga, In; X = Cl, Br, I; IPr = 1,3-bis(2,6-diisopropylphenyl)imidazol-2-ylidene; Y = weakly coordinating anion). These complexes can be isolated or generated in situ from $IPr{\cdot}MX_3$ and AgY. Since they display a single coordination site, we reasoned that they should be able to imitate the behavior of monocoordinating transition metal fragments and yield the conjugated product. Surprizingly, these species also gave rise to **2** selectively from **1** (Table 2, Entries 1 and 2). After realizing that actually no report mentioned the formation of **2** or **3** by transition metal-catalyzed cycloisomerization of **1**,[9] we tested it under Au(I) catalysis[10] and obtained again product **2** (Entry 3). However, with $IPr{\cdot}MX_2^+$ or Ph_3PAu^+ fragments, the coordination of the cyclopentene moiety to the metal center is unlikely.

Table 2. Ga(III)-, In(III)-, and Au(I)-Catalyzed Cycloisomerization of Enyne 1

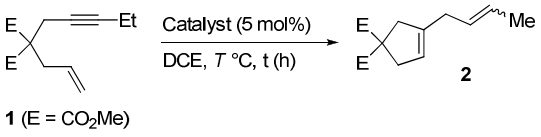

Entry	Catalyst	T [°C]	t [h]	E : Z[a]	Yield[b]
1	$[IPr{\cdot}GaCl_2][Al(pftb)_4]$[c]	80	4	8 : 1	32 (97)
2	$[IPr{\cdot}InBr_2][Al(pftb)_4]$[c]	80	2	4 : 1	42 (92)
3	$[Ph_3PAu][SbF_6]$[d]	20	1	4 : 1	50 (99)

[a] Determined by GLC analysis. [b] Corrected yield of **2** admixed with some unreacted **1**, conversion are indicated in parentheses. [c] Generated in situ from IPr·MX_3 (5 mol%) and $[Ag][Al(pftb)_4]$[11] (7 mol%); [d] Generated in situ from Ph_3PAuCl (5 mol%) and $AgSbF_6$ (7 mol%).

To address this discrepancy, we decided to test a different level of theory and then to take the *gem*-diester substitution into account. It is well-established that while the B3LYP functional usually lead to reliable geometries, better energies can be obtained with the Minnesota series of functionals.[12] Among them, the M06-2X performs very well for main group chemistry and non-covalent interactions.[13] The free energies shown in Table 1, Entry 3, have been obtained at the M06-2X/6-311+G(d,p) level. While the preference for the non-conjugated product remains clear with $GaCl_2^+$, it is no longer obvious that $GaCl_3$ would encourage the selective formation of the conjugated one, as the formation of products is expected to take place at very similar energy costs. Thus, the choice in the level of theory seems critical.

In fact, the model enyne used by Yu et al has not been tested experimentally.[14] It does not display the esters or the biphenyl group of **1** or **4**. Thus, we decided to use the real *gem*-diester tethered enyne **1** (E= CO_2Me) and the fluorene derivative **4** in the computations.[15] With the latter (Table 3), both BS3 (Entry 1) and BS4 (Entry 2), which is the same as BS3 with the LANL2DZ+ECP basis set for In, predict the correct isomer without invoking $InCl_2^+$ as active species. Moreover, with enyne **1**, only the formation of the non-conjugated diene could be modeled with M = $GaCl_3$ (Entry 1) and M = $InCl_3$ (Entry 2).

Table 3. M06-2X Free Energies of Activation (kcal/mol) of the Key Step of the MCl_3-Catalyzed Cycloisomerization of Enynes 4 (left) and 1 (right)

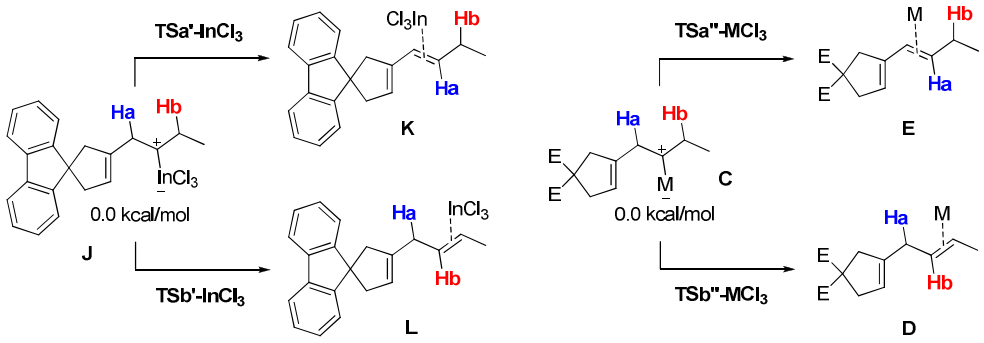

Entry	Basis set[a]	**TSa'-$InCl_3$**	**TSb'-$InCl_3$**	**TSa''-$GaCl_3$**	**TSb''-$GaCl_3$**	**TSa''-$InCl_3$**	**TSb''-$InCl_3$**
1	BS3	-	-	-[b]	4.7 [6.9][c]	-	-
2	BS4	10.2	7.2	-	-	-[b]	3.6 [6.2][c]

[a] BS3: 6-311+G(d,p) (all elements); BS4: 6-311+G(d,p) (C, H, O, Cl), LANL2DZ+ECP (In). [b] Not found. [c] Free energy of activation of the unassisted 1,2-Hb shift.

Interestingly, the geometry of the most stable transition states leading to the non-conjugated product varies greatly when esters are present in the tether (Figure 1). Alkane and fluorene tethered systems adopt a *trans* relationship between the migrating hydrogen and the cyclopentene framework (see **TSb-$GaCl_3$** and **TSb'-$InCl_3$**). On the other hand, a *cis* relationship is found in the *gem*-diester tethered transition states. The corresponding *cis* complexes have been computed as well and are significantly less stable by ~ 2.5 kcal/mol (see values in brackets in Table 3). The stabilization observed in the *cis* series is due to an interaction between the migrating hydrogen and one carbonyl oxygen. In O···H area, inspection of the maximum electron density reveals quite strong hydrogen bonds (ρ_{max} = 0.019 e.Å^{-3} and ρ_{max} = 0.023 e.Å^{-3} respectively for the Ga and In complexes). Thus, one ester group assists the [1,2]-H shift.

Figure 1. Selected Geometries of the Most Stable 1,2-Hb Migration Transition States (Distances in Å)

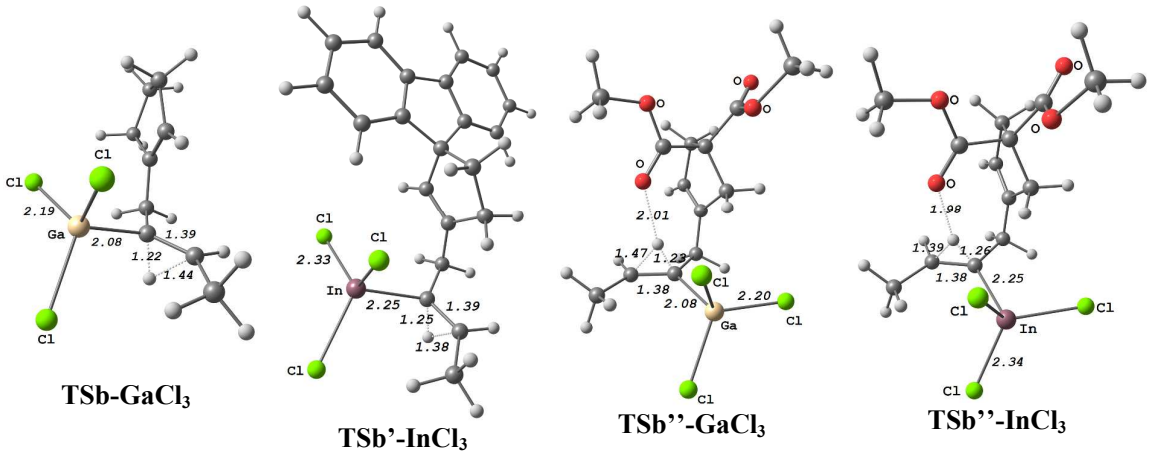

Our calculations on the "real" fluorene and *gem*-diester tethered systems show that there is no need to coordinate the C=C bond of the cyclopentene moiety to favor the migration of Hb and obtain the non-conjugated product thereof. This rapid re-examination of a previously studied reaction has revealed that the choice of the level of theory is critical and that over-simplifying the substrate in such computations can lead to conclusions at odds with experimental results. It has also shown that the presence of esters in the tether can favor specific conformations due to the presence of basic sites and lower activation barriers. Since there is at present no reason to invoke MX_2^+ ions as active species in MX_3-catalyzed transformations (M = Ga, In), $GaCl_3$ has been used in the next section.

2.2- $GaCl_3$-catalyzed Friedel-Crafts Reactions

It is well-established that Group 13 salts are exquisite catalysts for Friedel-Crafts reactions.[16] Among them, gallium(III) halides are often more efficient and safer catalysts than the corresponding aluminum salts.[17] Although a few computational studies on Group 13 halide-catalyzed Friedel-Crafts reaction of simple compounds (benzene, acetyl chloride, 2-chloropropane …) have been reported,[18] they reveal that the intimate mechanism is actually far more complex than anticipated. In particular,

the deprotonation steps are not the same in $AlCl_3$-catalyzed Friedel-Crafts acylation and alkylation.[18d] In both cases, the driving force to deprotonate the Wheland intermediate is the establishment of a strong hydrogen bond with the chlorine bridged counterion $Al_2Cl_7^-$ which plays the role of base. However, for the alkylation, an $Al_2Cl_7^-$-assisted [1,2]-H shift actually precedes the deprotonation. For Group 13 halide-catalyzed hydroarylation of alkynes, alkenes, and allenes, theoretical studies are also scarce and the deprotonation has not been studied.[8a,19] In this section, we investigate the mechanism of the $GaCl_3$-catalyzed hydroarylation of 1,6-arenynes and the subsequent bimolecular Friedel-Crafts reaction of the resulting dihydronaphthalenes with anisole.

It was previously reported that *gem*-diester tethered arenynes such as **6** undergo $GaCl_3$-catalyzed hydroarylation in 1,2-dichloroethane (DCE) at 80 °C to give bicyclic compounds such as **7** (Scheme 4).[3a] When the reaction of **6** or **7** is carried out in DCE or toluene at 80 °C in the presence of an aromatic nucleophile such as anisole, the adduct **8** is obtained.

Scheme 4. Ga(III)-Catalyzed Hydroarylation/Friedel Crafts Tandem of Arenyne 6

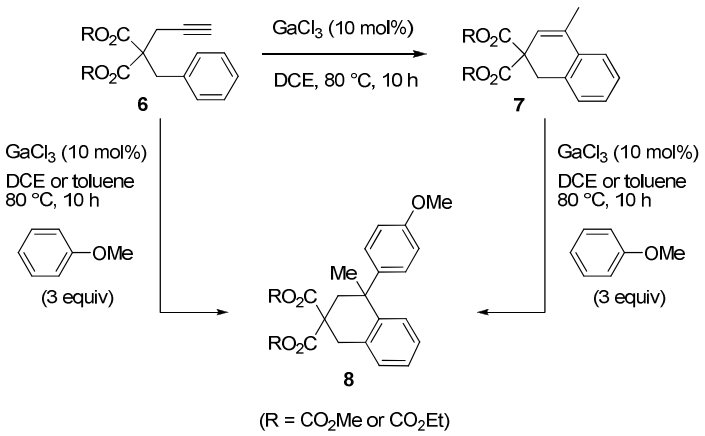

We have previously studied the hydroarylation mechanism by means of DFT computations at the B3LYP/LANL2DZ+ECP(Ga),6-31G(d) (other elements) level, including solvent correction for DCE.[8a] These results are summarized in Scheme 5. The coordination of the C≡C bond of **6** to give **9** triggers the nucleophilic attack of the benzene moiety to give **11** directly with a release of 43.6 kcal/mol of free energy. The transition state lies 13.6 kcal/mol above **9**. The expected Wheland

intermediate **10** did actually not converge. Dissociation of $GaCl_3$ and thermodynamically-driven exocyclic/endocyclic shift of the C=C bond provides **7**. The subsequent bimolecular Friedel-Crafts step has not been studied computationally.

Scheme 5. Previously Reported Relative Free Energies (ΔG_{298}, kcal/mol) for the Hydroarylation of 6 at the B3LYP/BS1 Level[8a] (a Value over an Arrow Corresponds to the Relative Free Energy of a Transition State)

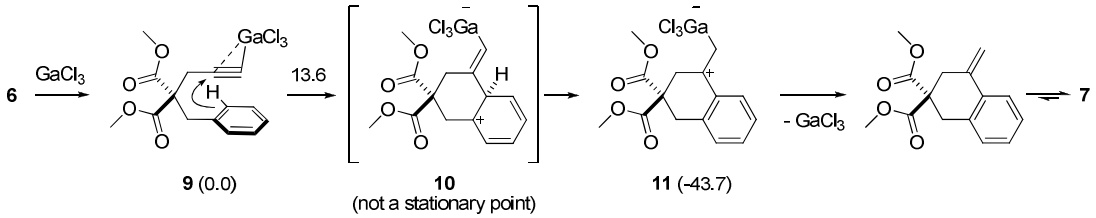

We decided to re-investigate the hydroarylation mechanism and to study the Friedel-Crafts step at the M06-2X/BS3 level (Scheme 6). To allow comparison with our previous results, solvent correction for DCE was included.

Scheme 6. Free Energy Profile of the Hydroarylation of Arenyne 6 (ΔG_{298}, kcal/mol) at the M06-2X/BS3 Level

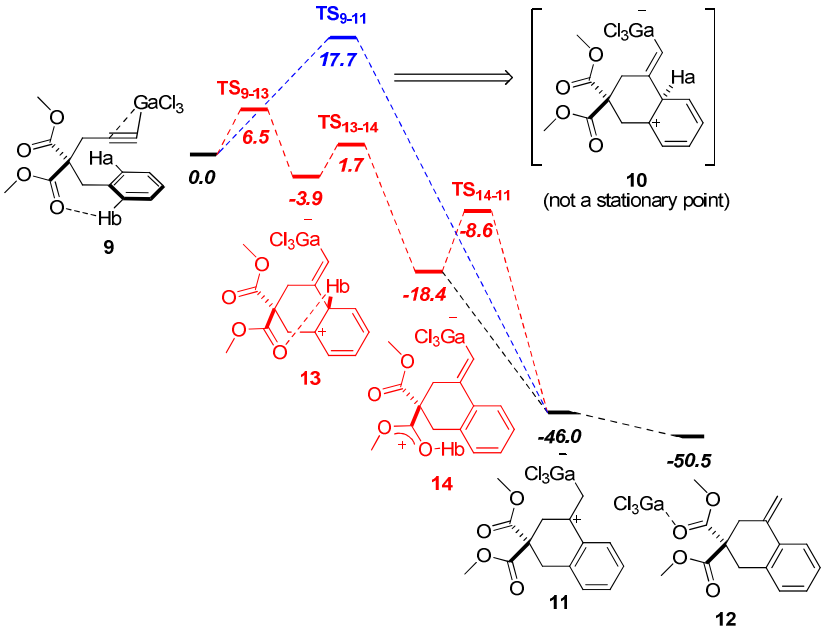

In the most stable isomer of **9**, the two carbonyls adopt an *anti* relationship (Figure 2). Therefore, the *ortho* hydrogens Ha and Hb of the benzene moiety are not equivalent and significant electron density indicative of a non-covalent interaction was found between Hb and the nearby carbonyl oxygen (O···Hb 2.41 Å, ρ_{max} = 0.011 e.Å^{-3}). The attack of the benzene carbon bearing Ha requires 17.7 kcal/mol of free energy of activation and leads, as in the B3LYP case mentioned above, to **11** without intermediate. This step is strongly exergonic by 46.0 kcal/mol. Migration of $GaCl_3$ from the carbon to one carbonyl oxygen results in a further release of 4.5 kcal/mol. If the Wheland intermediate had converged, its transformation into **11** would have been the result of two suprafacial [1,2]-H shifts instead of a symmetry forbidden [1,3]-H shift (Scheme 7).[19] Inspection of the transition vector of **TS$_{9-11}$** actually shows that it corresponds to the first [1,2]-H shift. Yet neither **10** nor **10'** are stable and collapse to **11** in the forward direction and to **9** in the backward direction.

Scheme 7. Resemblance Between TS$_{9-11}$ and the Fictive TS$_{10-10'}$

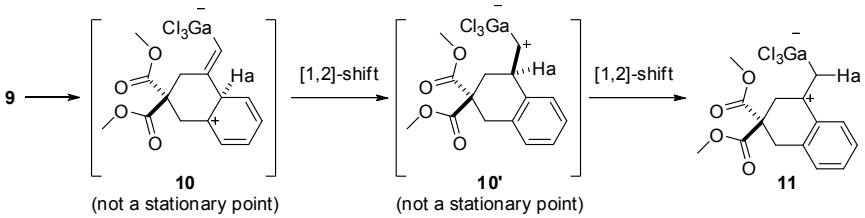

The attack of the carbon bearing Hb proceeds quite differently. It leads to the Wheland intermediate **13** which is formed in an exergonic fashion (ΔG_{298} = -3.9 kcal/mol) through a transition state that lies only 6.5 kcal/mol above **9**. In **13**, the O···Hb distance is only 2.09 Å and ρ_{max} increases to 0.019 e.Å^{-3}. Migration of Hb to O is achieved through a low-lying transition state ($\Delta G^{\ddagger}_{298}$ = 5.6 kcal/mol for this step) and **14** is formed in an appreciably exergonic fashion (ΔG_{298} = -14.5 kcal/mol). The shift of Hb from O to the carbon bearing the gallium atom is also straightforward as far as the free energy of activation is concerned ($\Delta G^{\ddagger}_{298}$ = 9.8 kcal/mol) and it is strongly exergonic (ΔG_{298} = -27.6 kcal/mol).[20,21]

Figure 2. Geometries of the Computed Species Shown in Scheme 6 (Distances in Å)

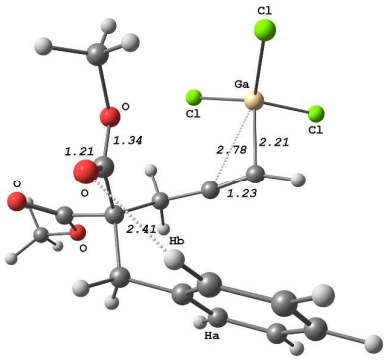

9

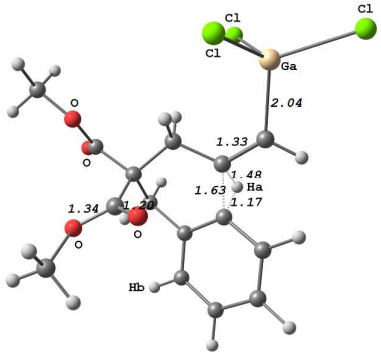

$TS_{9\text{-}11}$

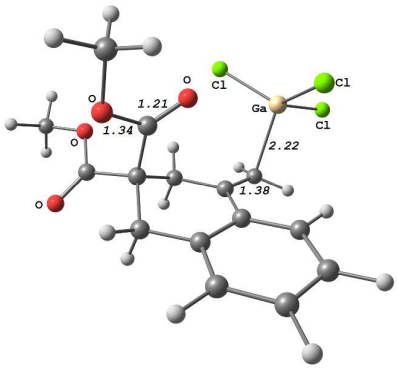

11

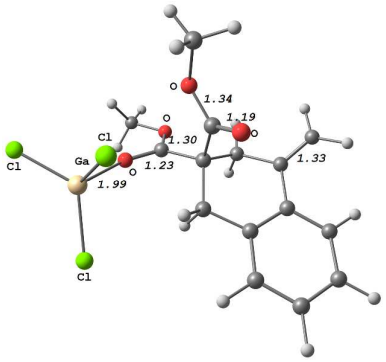

12

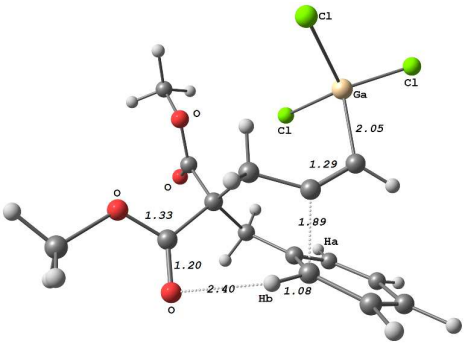

$TS_{9\text{-}13}$

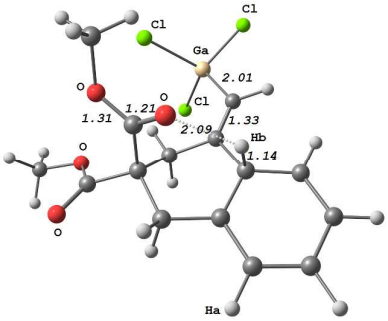

13

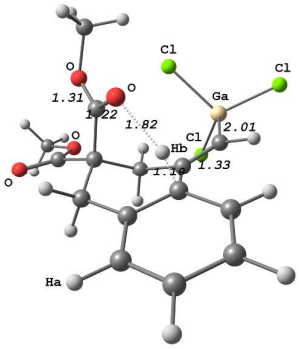

$TS_{13\text{-}14}$

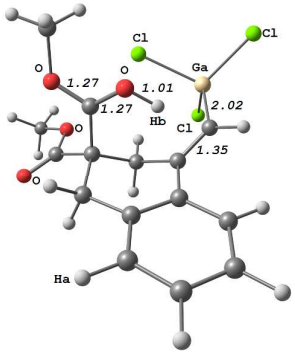

14

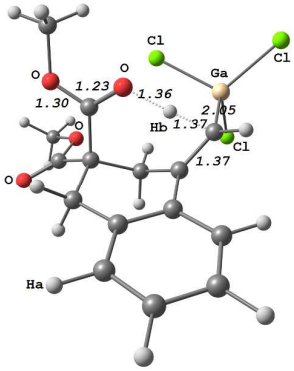

$TS_{14\text{-}11}$

The Friedel-Crafts reaction was studied next (Scheme 8 and Figure 3). Here again, we found two pathways to reach compound **8** shown in Scheme 4 (i.e. **17** in Scheme 8 with $GaCl_3$ coordinated to one carbonyl oxygen of **8**). The first one does not involve the esters (path 1). Complex **11** and anisole transform through a relatively low-lying transition state ($\Delta G^{\ddagger}_{298}$ = 6.1 kcal/mol) into the Wheland intermediate **15** in a virtually athermic fashion. A proton transfer giving rise to the σ-complex **16**[22] and then the O-coordinated complex **17** was computed. Despite the downhill nature of this sequence (ΔG_{298} = -12.6 kcal/mol to **16** and then -21.7 kcal/mol from **16** to **17**), the [1,3]-H shift requires a high free energy of activation of 33.9 kcal/mol.

Scheme 8. Free Energies Profile of the Friedel-Crafts Step of the Tandem Transformation of Arenyne 6 (ΔG_{298}, kcal/mol) at the M06-2X/BS3 Level

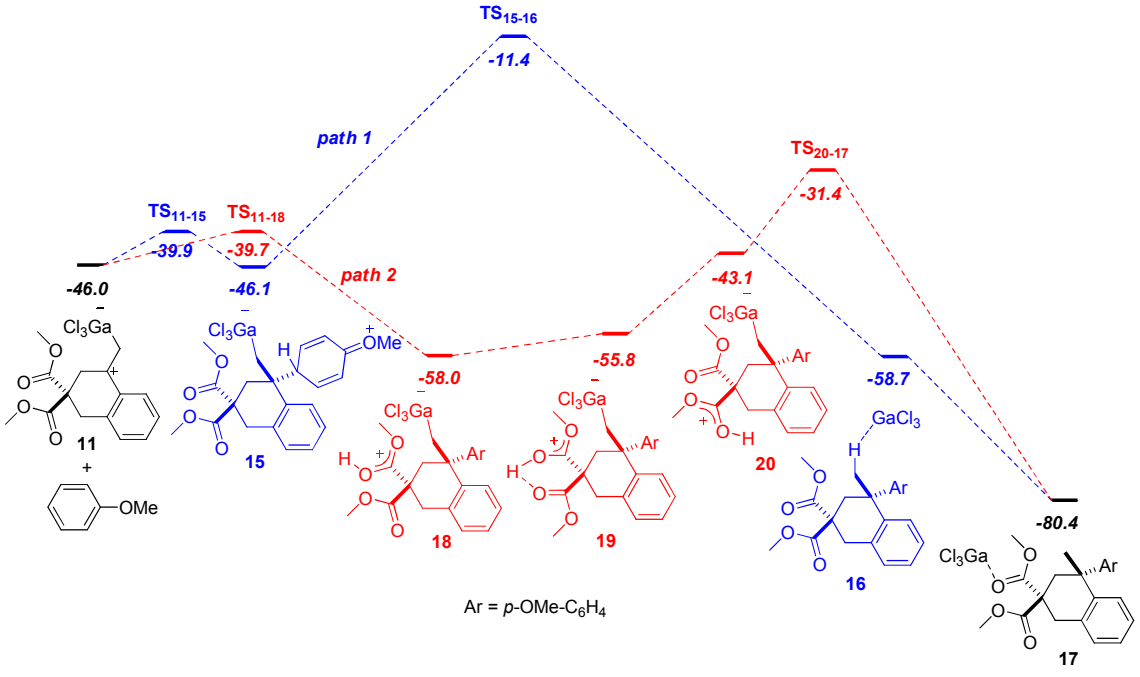

Alternatively, **11** can react with anisole in a process which involves the simultaneous C-C bond formation and cleavage of the C-H bond (path 2). One carbonyl oxygen of **11** serves as base to deprotonate anisole which is found already aromatic in **18**. Concerted S_EAr mechanisms for arene sulfonation[23] and chlorination[24] have been computed and refute the traditional text-book perspective of Friedel-Crafts reactions systematically involving Wheland σ-complexes. However, the possibility of concerted Friedel-Crafts alkylation involving a three-centered transition state is unknown to us (Scheme 9).

Scheme 9. Possible concerted Friedel-Crafts alkylation

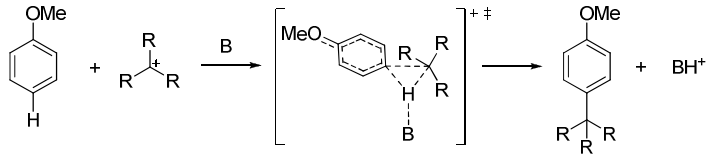

The free energy of activation of the concerted S_EAr is virtually the same as the one to reach **15**. Isomers of **18** in which the proton is shared by the two carbonyl oxygen atoms (**19**) or is fixed at the one *cis* to the $GaCl_3$ fragment (**20**) were computed, yet they are less stable than **18**. Nevertheless, from **20**, oxygen-to-carbon migration can occur. The transition state of this protodemetallation step lies much lower in free energy than the one from **15** to **16** (-31.4 vs -11.4 kcal/mol). Therefore, the ester-assisted addition of anisole to **11** is the most favorable pathway.

Figure 3. Geometries of the Computed Species Shown in Scheme 8 (Distances in Å)

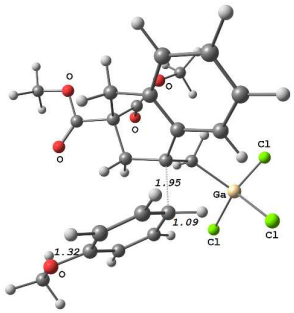

$TS_{11\text{-}15}$

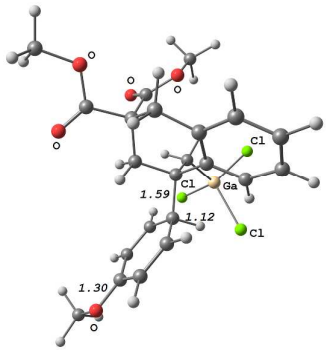

15

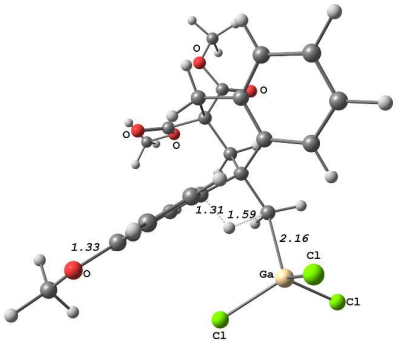

$TS_{15\text{-}16}$

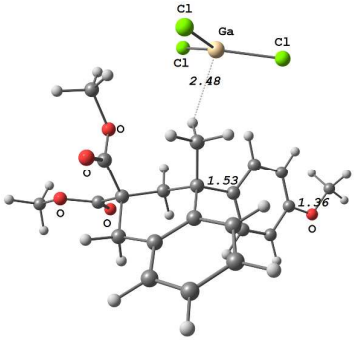

16

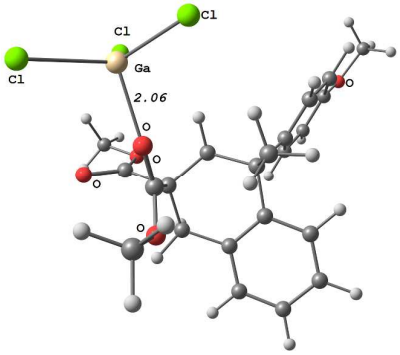

17

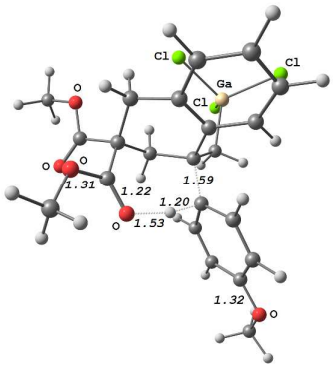

$TS_{11\text{-}18}$

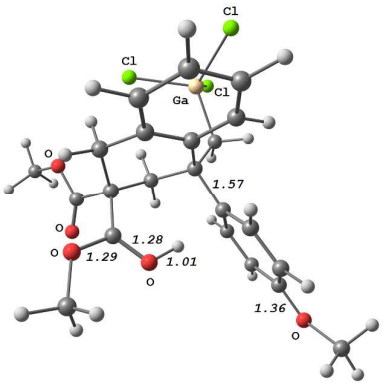

18

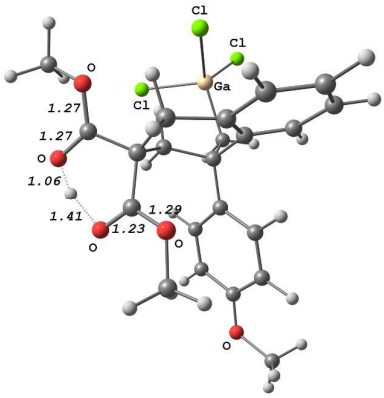

19

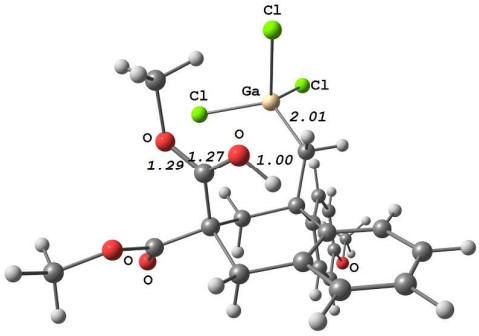

20

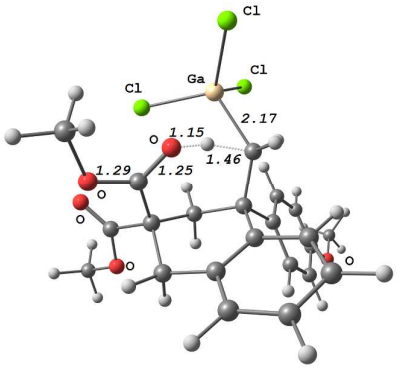

$TS_{20\text{-}17}$

One could argue that the proton migration could take place in an intermolecular solvent-mediated fashion, yet the above reaction works equally well in toluene.[8a] Another possibility would be a bimolecular process between two reaction intermediates; however, this scenario was ruled out by the study of the reactivity of a substrate that does not display hydrogen bond acceptor functionalities: the fluorene derivative **21** (Scheme 10). When submitted to $GaCl_3$ in DCE or toluene, the hydroarylation took place but not the Friedel-Crafts step.

Scheme 10. Ga(III)-Catalyzed Hydroarylation of Arenyne 21

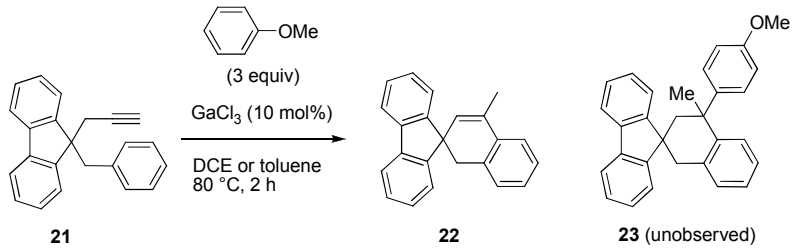

Computations rationalize this feature (Scheme 11 and Figure 4). The hydroarylation proceeds in a concerted fashion through a low-lying transition state ($\Delta G^{\ddagger}_{298}$ = 8.5 kcal/mol).[25] The formation of **25** is strongly exergonic (ΔG_{298} = -48.6 kcal/mol). That of the Wheland intermediate **26** requires a modest free energy of activation of 5.7 kcal/mol and is endergonic by 2.8 kcal/mol. Again, the protodemetallation step (**26** to **27** and then **28**), although strongly exergonic (ΔG_{298} = -9.2 kcal/mol and then -25.2 kcal/mol) is compromised by a high activation barrier of 30.0 kcal/mol. Since there is no basic sites in the substrates, there is no alternative route.

Scheme 11. Free Energy Profile of the Hydroarylation/Friedel-Crafts Transformation of Arenyne 21 (ΔG_{298}, kcal/mol) at the M06-2X/BS3 Level

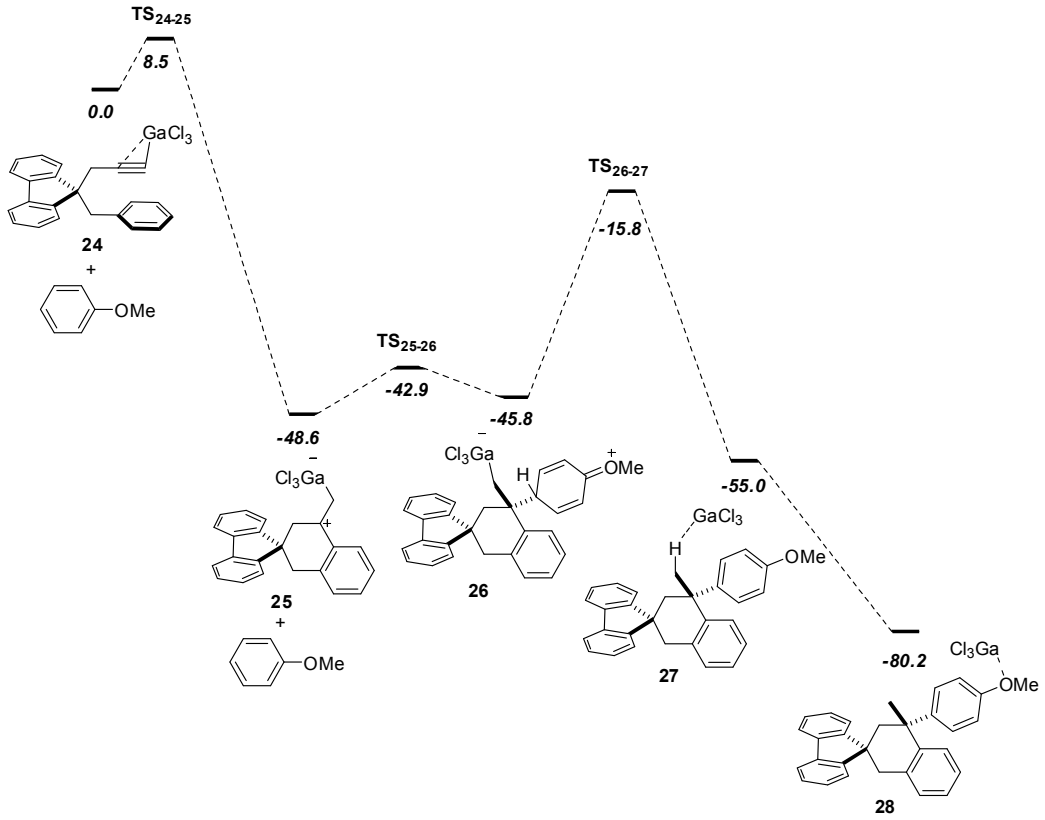

Figure 4. Geometries of the Computed Species Shown in Scheme 11 (Distances in Å)

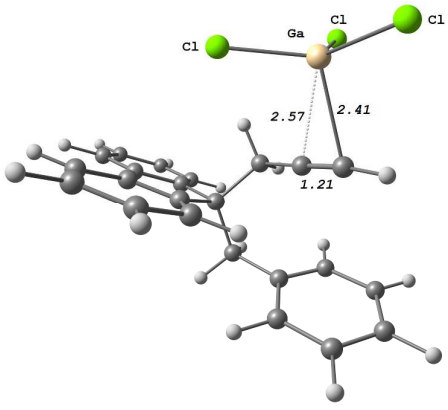

24

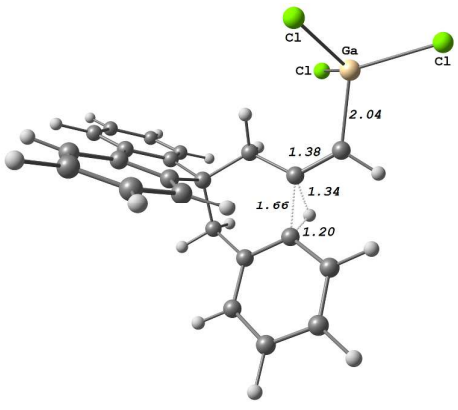

$TS_{24\text{-}25}$

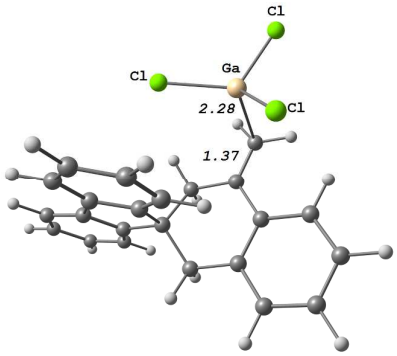

25

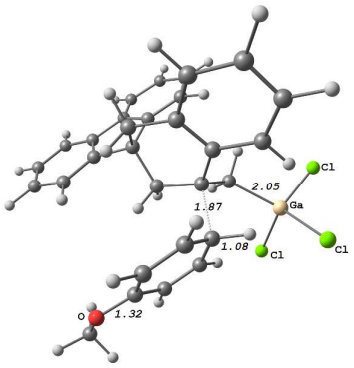

$TS_{25\text{-}26}$

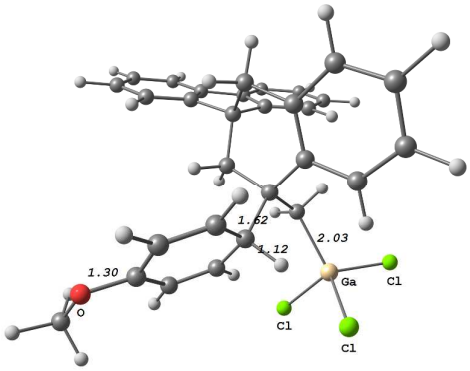

26

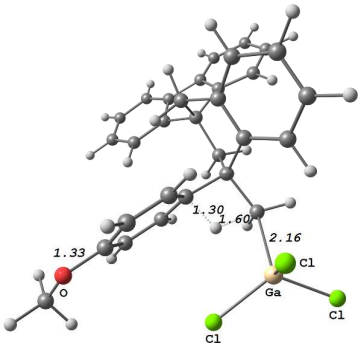

$TS_{26\text{-}27}$

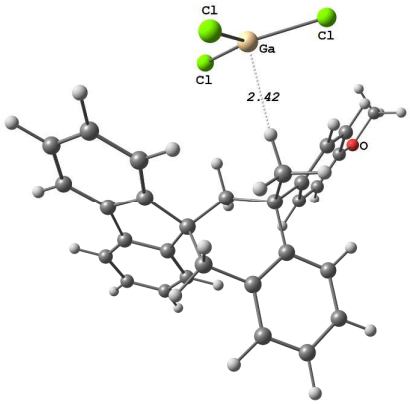

27

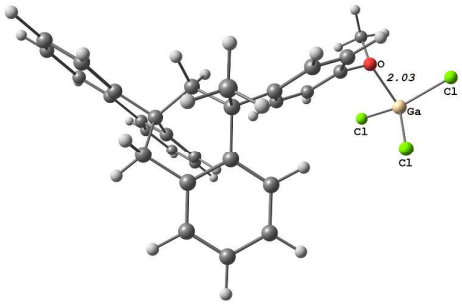

28

Even though the calculations presented in Sections 2.1 and 2.2 are restricted to Group 13 metal-catalyzed reactions involving *gem*-diester tethered substrates, there is no reason to believe that the conclusions reached would not apply to other kind of transformation involving a proton transfer, as long as a functional group such as an ester is well enough located to shuttle the migrating hydrogen.

To address this issue, we have next studied a platinum(II)-catalyzed reaction in which the substrate does not display a *gem*-diester tether, but a simple ester substituent at the reacting alkyne unit of an arenyne.

2.3- $PtCl_2$-Catalyzed Hydroarylation of 1,6-Arenynes

In this section, we turn our attention to the hydroarylation of biphenylacetylenes described by Fürstner[26] for the following reasons: *i*) not only main group metal salts but also transition metal complexes such as $PtCl_2$ are known to be active catalysts for this transformation; *ii*) the cyclization of a substrate displaying a single ester group has been carried out; *iii*) the mechanism has already been studied by Soriano but the possibility of ester-assisted proton transfer has not been considered.[19] In fact, the cyclization of such substrates can lead to fluorenes or phenanthrenes, the latter type being the major one when $PtCl_2$ is used as catalyst, except with an ester at the alkyne terminus as in **29** (Scheme 12). In this case, the fluorene derivative **30** is formed selectively as an *E*/*Z* mixture.

Scheme 12. Platinum-Catalyzed Cycloisomerization of Compound 29

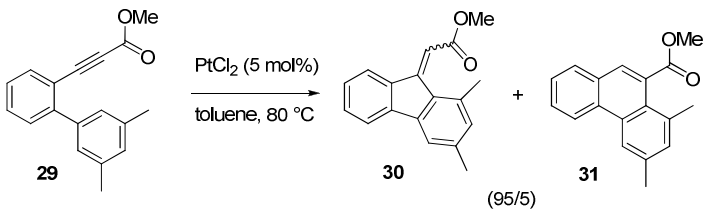

From B3LYP/LANL2DZ+ECP(Pt),6-31G(d) (other elements) computations using on a simplified model substrate, Soriano and Marco-Contelles proposed a mechanism involving a 5-*exo*-dig or a 6-*endo*-dig attack of the arene onto the complexed C≡C bond, followed by two [1,2]-H shifts. They showed that the reversal of selectivity between the 5-*exo* and the 6-*endo* pathways was due to the polarization of the C≡C bond induced by the ester. The preference for the 5-*exo*-dig cyclization was

shown on the "real" substrate **29**, but the [1,2]-H shifts were not computed in this case. Intrigued by the proximity of the carbonyl group with the migrating proton in complex **33**, we decided to compare the [1,2]-H shifts sequence with an ester-assisted proton transfer (Scheme 13 and Figure 5). From our part, we used the B3LYP/LANL2DZ+ECP(Pt),6-311+G(d,p) (other elements) level for the geometry optimizations and to get the thermal corrections to the free energies. We then carried out single point calculations using the M06 functional, the SDD basis set for Pt, and the 6-311+G(d,p) basis set for other elements. A barrier of 18.2 kcal/mol was computed for the transformation of starting complex **32** into the Wheland intermediate **33**, which represents the rate determining step. From **33**, 13.3 kcal/mol of activation energy are required to give the platinum carbenoid **34**. The second [1,2]-H shift leading to the complexed alkene **35** is achieved at a free energy cost of 23.9 kcal/mol. The entire sequence is downhill with a total exergonicity of 25.3 kcal/mol. From **33**, the capture of the proton proceeds straightforwardly through a 7.4 kcal/mol activation barrier. A virtually barrierless rotation of the protonated ester in **36** yields **37**, which is greatly stabilized by an OH···Cl hydrogen bond. Protodemetallation finally takes place through a 20.4 kcal/mol activation barrier to give **38**, which is actually the diastereomer of **35**. Indeed, the migration of the proton to the metallated carbon atom requires rotation of the C=C bond. The overall **33→38** process is also downhill and is kinetically favored over the **33→35** pathway.

Scheme 13. Free Energy Profile of the Hydroarylation of Arenyne 32 (ΔG_{298}, kcal/mol) at the M06 Level

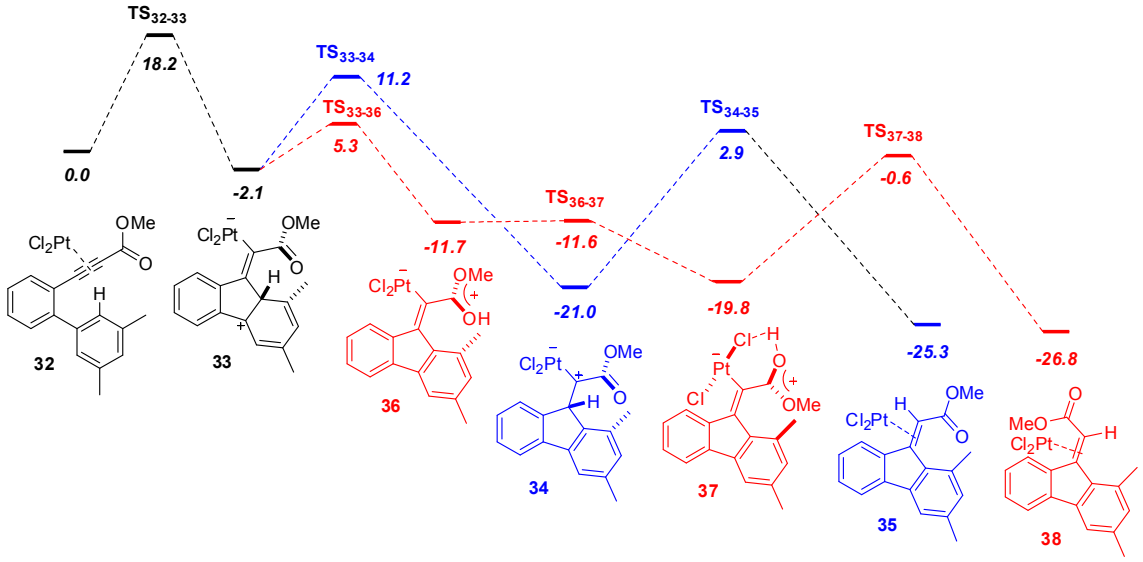

Figure 5. Geometries of the Computed Species Shown in Scheme 13 (Distances in Å)

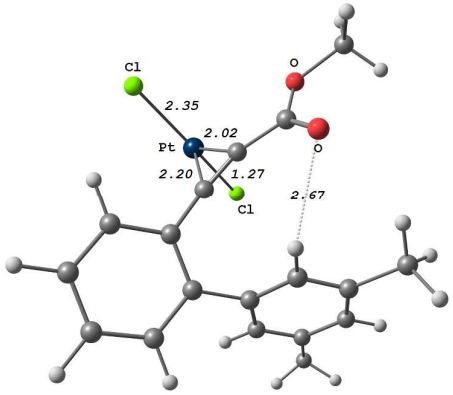

32

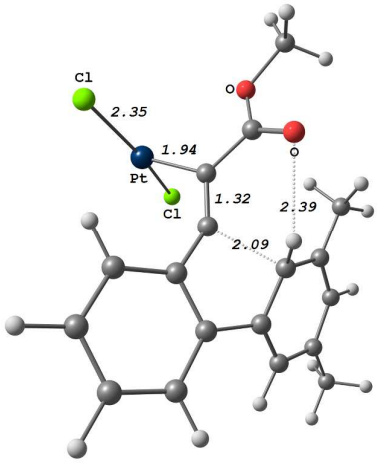

TS_{32-33}

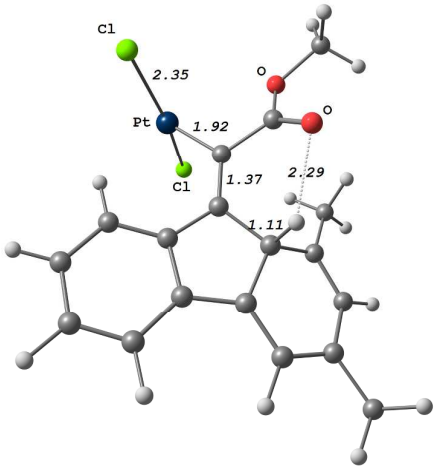

33

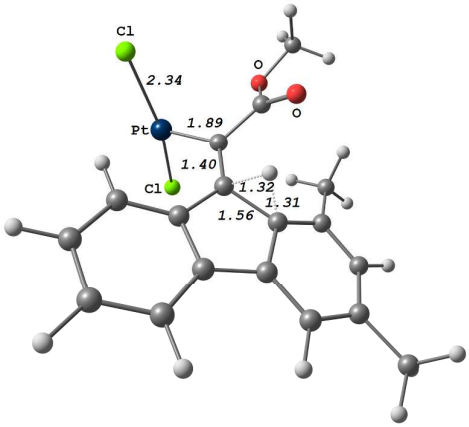

TS_{33-34}

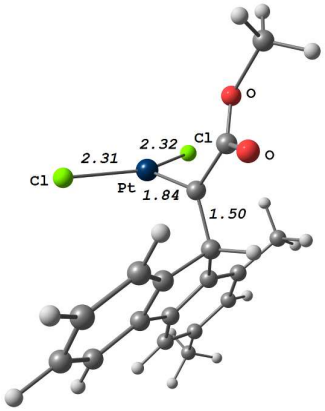

34

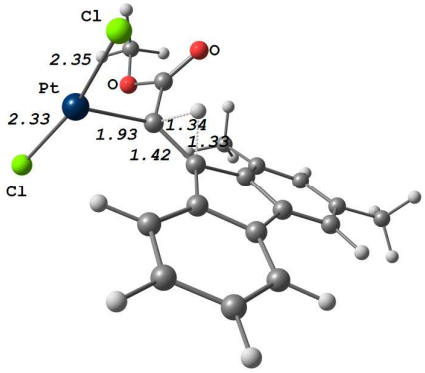

TS_{34-35}

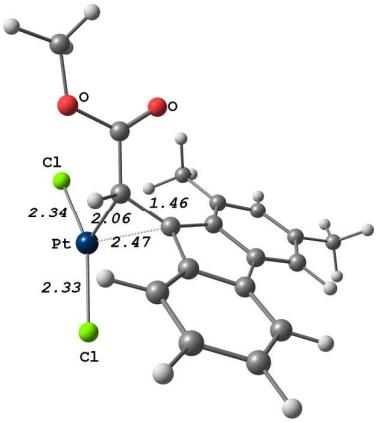

35

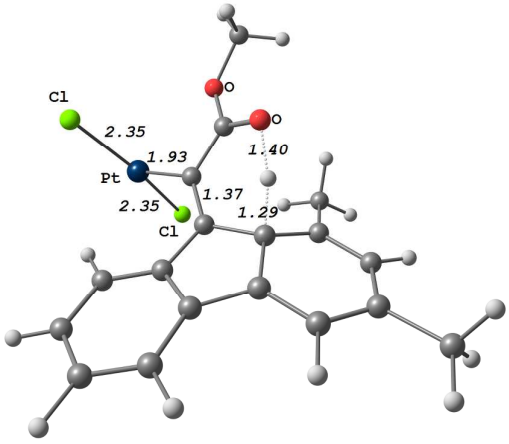

TS_{33-36}

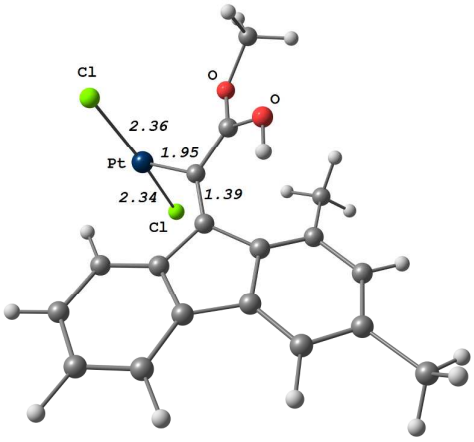

36

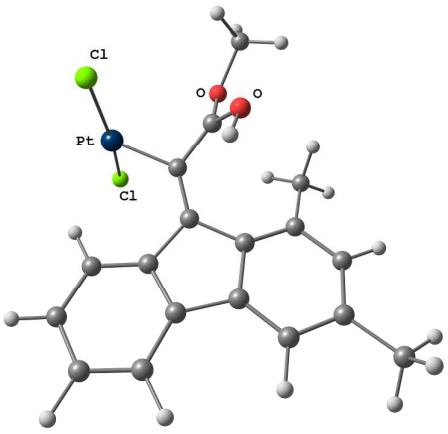

$TS_{36\text{-}37}$

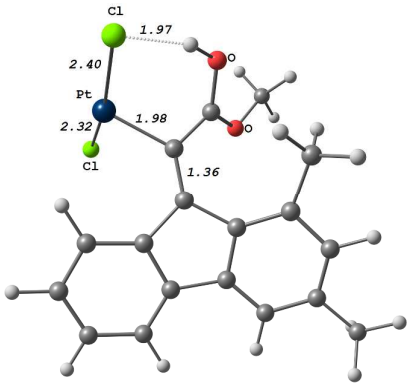

37

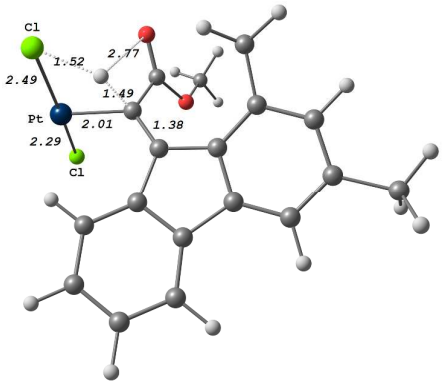

$TS_{37\text{-}38}$

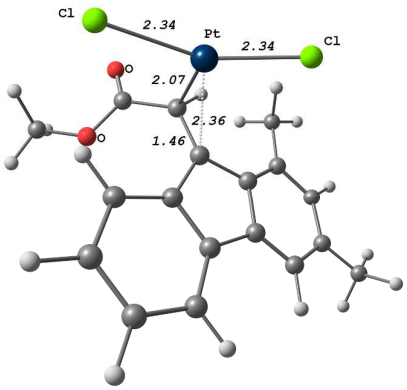

38

Thus, the ester group at the alkyne enables a mechanistic alternative. It can serve as proton carrier to ensure the rearomatization of the Wheland intermediate and the protodemetallation step.

3- Conclusion

The above computations indicate that the ester functionality can play an active chemical role in metal-catalyzed carbocyclization and Friedel-Crafts reactions by shuttling protons from one place to another. In particular, a rare kind of concerted S_EAr where the ester functionality acts as base has been uncovered. While the ability of carbonyls to transfer hydrogens is well-known in the coordination sphere of a metal (for instance inner sphere pivalate-assisted concerted metalation deprotonation (CMD)),[27] it is overlooked in metal-catalyzed reactions occurring under substrate control.

4- Experimental Section

Computations. All the calculations were performed using the GAUSSIAN 09 software package.[28] For the study of gallium- and indium-catalyzed reactions, the structures were optimized and characterized to be energy minima (no imaginary frequency) or transition states (one imaginary frequency) at the M06-2X[29] level. The 6-311+G(d,p)[30] basis set (BS3) was used for C, H, N, Cl, O, and Ga, and the LANL2DZ+ECP[31] basis set was used for In (BS4). The thermal corrections to free energies were carried out at 298.15 K and 1 atm using the M06-2X harmonic frequencies (ΔG_{298}). Solvent corrections to the free energies were obtained for 1,2-dichloroethane (DCE) with the CPCM model.[32] For the study of the platinum-catalyzed reaction, computations were carried out at the B3LYP[33] level using the LANL2DZ+ECP[31] basis set for Pt and the 6-311+G(d,p)[30] basis set for the other elements. Single point calculations using the B3LYP optimized geometries were carried out with the M06[29] functional and a larger basis set of SDD[34] for Pt. The thermal corrections to free energies were obtained at 298.15 K and 1 atm using the B3LYP harmonic frequencies (ΔG_{298}).

General Information. All reactions were performed in oven-dried flasks under argon atmosphere. Unless otherwise stated, commercially available reagents were used as received without further purification. Gallium, and indium halides were obtained from Alfa Aesar and used as received. Silver hexafluoroantimonate was purchased from Sigma-Aldrich and used as received. 1,2-Dichloroethane was distilled from calcium hydride and degassed by Freeze-Pump-Thaw technique. Unless otherwise

stated, products were purified by chromatography over silica gel. TLC plates were visualized by UV light (254 nm) and *p*-anisaldehyde staining. GC analysis was performed with a non-polar column (15 m x 0.25 mm x 0.25 mm) NMR spectra were recorded on 360 and 300 MHz spectrometers. Chemical shifts are reported in parts per million (ppm). The spectra were referenced to the residual ^{1}H and ^{13}C signals of the solvents as follows: $CDCl_3$ (^{1}H, δ = 7.27 ppm; ^{13}C, δ = 77.0 ppm). Data are given in the following order: chemical shift, multiplicity (s = singlet, d = doublet, m = multiplet), coupling constant (*J*) in Hz and integration. Infrared spectra were recorded on a FTIR spectrometer (KBr pellets) and are reported in cm^{-1}. HRMS were performed by electrospray ionization using a qTOF mass spectrometer. IPr·$GaCl_3$, [35] IPr·$InBr_3$, [36] and [Ag][Al(pftb)$_4$][11] were prepared following reported procedures. Enyne **1** was synthesized according to a previously described method.[4a] Arenyne **6** was prepared following a reported procedure.[8a,8b] The synthesis and characterization of compounds **7** and **8** were previously reported by our team.[8a] Arenyne **21** and cycloalkene **22** were also described previously.[8b]

Procedures for the Cycloisomerization of Enyne 1

General considerations: the substantial difference between conversions and isolated yields can be explained by polymerization occurring as side reactions. Thus, rinsing silica gel with Et_2O after flash chromatography leads to the recovery of the missing material as a very complex mixture. These complex mixtures were already observed by ^{1}H-NMR analysis of the crude product before the purification step. Also, as Yu *et coll.* have previously stated,[4a] the generated dienes are stable on silica gel. Moreover, no other isomers arising from **1** could be observed by GC monitoring. The NMR spectra of **2** displayed in the Supporting Information were obtained from condition B as a representative outcome of a main-group metal-catalyzed cycloisomerization of **1**.

Condition A: IPr·$GaCl_3$ (5 mol%, 0.0125 mmol, 7.06 mg) was dissolved in DCE (0.5 mL) in a screw-cap vial under argon. [Ag][Al(pftb)$_4$] (7 mol%, 0.0175 mmol, 18.81 mg) was added and the mixture was stirred for 5 min. A solution of enyne **1** (0.25 mmol, 59.6 mg) in DCE (0.5 mL) was added and the reaction mixture was stirred at 80 °C for 4 h. After filtration over a short pad of Celite

and evaporation of the solvent, the crude residue was purified by chromatography over silica gel (10% AcOEt in pentane) to afford a mixture of **1**, **2**-*E* and **2**-*Z* (21 mg) in 32% corrected yield of **2**. The ratio indicated in Table 4 was determined by GC. 97% conversion was determined based on the recovery of 3% of **1**.

Condition B: IPr·$InBr_3$ (5 mol%, 0.0125 mmol, 9.31 mg) was dissolved in DCE (0.5 mL) in a screw-cap vial under argon. [Ag][Al(pftb)$_4$] (7 mol%, 0.0175 mmol, 18.81 mg) was added and the mixture was stirred for 5 min. A solution of enyne **1** (0.25 mmol, 59.6 mg) in DCE (0.5 mL) was added and the reaction mixture was stirred at 80 °C for 2 h. After filtration over a short pad of Celite and evaporation of the solvent, the crude residue was purified by chromatography over silica gel (10% AcOEt in pentane) to afford a mixture of **1**, **2**-*E* and **2**-*Z* (30 mg) in 42% corrected yield of **2**. The ratio indicated in Table 4 was determined by GC. 92% conversion was determined based on the recovery of 8% of **1**.

Condition C: Ph_3PAuCl (5 mol%, 0.0125 mmol, 6.18 mg) was dissolved in DCE (0.5 mL) in a screw-cap vial under argon. $AgSbF_6$ (7 mol%, 0.0175 mmol, 6.01 mg) was added and the mixture was stirred for 5 min. A solution of enyne **1** (0.25 mmol, 59.6 mg) in DCE (0.5 mL) was added and the reaction mixture was stirred at room temperature for 1 h. After filtration over a short pad of Celite and evaporation of the solvent, the crude residue was purified by chromatography over silica gel (10% AcOEt in pentane) to afford a mixture of **2**-*E* and **2**-*Z* (30 mg) in 50% yield. The ratio indicated in Table 4 was determined by GC.

Table 4. Ratio of enyne **1** and dienes **2**-*E* and **2**-*Z* determined by GC analysis.

Condition	**1** [Area%]	**2**-*E* [Area%]	**2**-*Z* [Area%]	Ratio [**1** : **2**-*E* : **2**-*Z*]
A	9.87	78.45	11.68	1 : 8 : 1
B	15.26	69.66	15.08	1 : 4 : 1
C	0	81.35	18.65	0 : 4 : 1

Method: 50 °C (1 min), slope 10 °C.min^{-1} (20 min), 250 °C (2 min). GC retention time: 9.9 min (**1**), 10.9 min (**2**-*E*), 11.1 min (**2**-*Z*).

(*E*)-Dimethyl 3-(but-1-en-1-yl)cyclopent-3-ene-1,1-dicarboxylate and (*Z*)-dimethyl 3-(but-1-en-1-yl)cyclopent-3-ene-1,1-dicarboxylate 2:

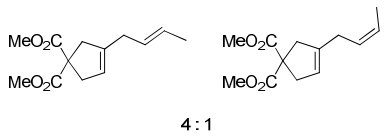

Obtained following condition B (Table 1, entry 2). Colorless oil; **2**-*E* : **2**-*Z* = 4 : 1 determined by GLC analysis. NMR of the major isomer **2**-*E*: ^{1}H NMR (360 MHz, $CDCl_3$) δ 5.52 – 5.38 (m, 2H), 5.22 (m, 1H), 5.10 – 5.19 (m, **2**-*Z*), 3.73 (s, 8.4H, **2**-*E* and **2**-*Z*), 2.99 (m, 2.7H, **2**-*E* and **2**-*Z*), 2.92 (m, 2.7H, **2**-*E* and **2**-*Z*), 2.80 – 2.75 (m, **2**-*Z*), 2.72 (m, 2H), 1.66 (d, J = 5.4 Hz, 3H), 1.61 (d, J = 6.5 Hz, **2**-*Z*); ^{13}C NMR (90 MHz, $CDCl_3$) δ 172.7, 140.9, 127.6, 126.7, 120.7, 59.0, 52.8, 43.0, 40.7, 33.9, 17.8; FT-IR (film): ν 1736, 1434, 1256, 1194, 1160, 1070, 966 cm^{-1}; HRMS (ESI) *m/z*: calcd for $C_{13}H_{18}O_4Na$ $[M + Na]^+$: 261.1097 found: 261.1095. The data correspond to those previously described in the litterature.[4a]

Procedure for the Hydroarylation of Arenyne 21:

A solution of arenyne **21** (0.125 mmol, 36.8 mg) and anisole (0.75 mmol, 41 µL) in DCE or toluene (0.5 mL) was added to $GaCl_3$ (10 mol%, 0.0125 mmol, 2.2 mg) in a screw-cap vial under argon. The reaction mixture was stirred at 80 °C for 2 h (full conversion was observed by TLC monitoring). After filtration over a short pad of silica gel (CH_2Cl_2), solvents were evaporated under vacuum. The yield of **22** was then determined by ^{1}H NMR analysis after the addition of one equivalent of *p*-anisaldehyde (0.125 mmol, 15.2 µL) as internal standard. 54% of **22** was obtained when the reaction was performed in DCE and 87% of **22** was obtained when the reaction was performed in toluene. The Friedel-Crafts adduct **23** was not observed in either case.

Acknowledgements: This work was supported by UPS, IUF, and CNRS. We used the computing facility of the CRIHAN (project 2006-013)

Supporting Information: NMR spectra of **2**, energies and coordinates of the computed intermediates. This material is available free of charge via the Internet at http://pubs.acs.org/."

References:

(1) Jung, M. E.; Piizi, G. *Chem. Rev*. **2005**, *105*, 1735.

(2) (a) Michelet, V.; Toullec, P. Y.; Genêt, J.-P. *Angew. Chem. Int. Ed*. **2008**, *47*, 4268. (b) Herrero-Gómez, E.; Echavarren, A. M. In *Handbook of Cyclization Reactions*, Shengming, M. Ed; **2010**, *2*, 625. (c) Aubert, C.; Fensterbank, L.; Garcia, P.; Malacria, M.; Simonneau, A. *Chem. Rev*. **2011**, *111*, 1954. (d) Yamamoto, Y. *Chem. Rev*. **2012**, *112*, 4736. (e) Michelet, V. In *Comprehensive Organic Synthesis* (2nd Edition), Knochel, P.; Molander, G. A, Eds; **2014**, *5*, 1483.

(3) (a) Inoue, H.; Chatani, N.; Murai, S. *J. Org. Chem.* **2002**, *67*, 1414. (b) Chatani, N.; Inoue, H.; Kotsuma, T.; Murai, S. *J. Am. Chem. Soc*. **2002**, *124*, 10294. (c) Mamane, V.; Hannen, P.; Fürstner, A. *Chem. Eur. J.* **2004**, *10*, 4556. (d) Simmons, E. M.; Sarpong, R. *Org. Lett*. **2006**, *8*, 2883.

(4) (a) Zhuo, L.-G.; Zhang, J.-J.; Yu, Z.-X. *J. Org. Chem*. **2012**, *77*, 8527. (b) Zhuo, L.-G.; Zhang, J.-J.; Yu, Z.-X. *J. Org. Chem*. **2014**, *79*, 3809. (c) Zhuo, L.-G.; Shi, Y.-C.; Yu, Z.-X. *Asian J. Org. Chem*. **2014**, *3*, 842.

(5) Miyanahana, Y.; Chatani, N. *Org. Lett*. **2006**, *8*, 2155.

(6) The values presented here come from the Supporting Information of Ref. 4c. They are different from those presented in the article. Surprizingly the authors did not use the free energy values of their most stable isomers. Also the depicted transition states do not always correspond to the discussed series. By using the right values, we reached the same conclusions nonetheless.

(7) The reaction of dimethyl cyclopropane-1,1-dicarboxylate with $GaCl_3$ yields the expected molecular adduct with no ionization of the Ga-Cl bond: Novikov, R. A.; Balakirev, D. O.; Timofeev, V. P.;

Tomilov, Y. V. *Organometallics* **2012**, *31*, 8627. ^{71}Ga NMR did not reveal the typical sharp signal of $GaCl_4^-$.

(8) (a) Li, H.-J.; Guillot, R.; Gandon, V. *J. Org. Chem*. **2010**, *75*, 8435. (b) Michelet, B.; Bour, C.; Gandon, V. *Chem. Eur. J.* **2014**, *20*, 14488. (c) Michelet, B.; Colard-Itté, J.-R.; Thiery, G.; Guillot, R.; Bour, C.; Gandon, V. *Chem. Commun.* **2015**, *51*, 7401; and references cited therein.

(9) Cycloisomerization of **1** into dienes under transition metal catalysis has been reported twice but products **2** and **3** were not observed: (a) Kezuka, S.; Okado, T.; Niou, E.; Takeuchi, R. *Org. Lett;* **2005**, *7*, 1711. (b) Kondo, T.; Suzuki, N.; Okada, T.; Mitsudo, T.-a. *J. Am. Chem. Soc.* **1997**, *119*, 6187.

(10) Hashmi, A. S. K.; Hutchings, G. J. *Angew. Chem. Int. Ed*. **2006**, *45*, 7896.

(11) Since $[Al(pftb)_4]$ it is one the most weakly coordinating anion, it is unlikely to interfere in the reaction process. See: Krossing, I. *Chem. Eur. J*. **2001**, *7*, 490.

(12) Häller, L. J. L.; MacGregor, S. A.; Panetier, J. A. In N-Heterocyclic Carbenes: From Laboratory Curiosities to Efficient Synthetic Tools, RSC Catalysis Series, Díez-González, S. Ed, 2011, pp 42-76.

(13) Zhao, Y.; Truhlar, D. G. *Theor. Chem. Acc*. **2008**, *120*, 215.

(14) It should be difficult to synthesize and the reaction products difficult to separate from the substrate.

(15) Only the most stable isomer is presented in each case.

(16) See inter alia: Olah, G. A.; Farooq, O; Farnia, S. M. F., Olah, J. A. *J. Am. Chem. Soc*. **1988**, *110*, 2560.

(17) See inter alia: Matuszek, K.; Chrobok, A.; Hogg, J. M.; Coleman, F.; Swadźba-Kwaśny, M. *Green Chem.* **2015**, *17*, 4255 and the references therein.

(18) (a) Tarakeshwar, P.; Lee, J. Y. Kim, K. S. *J. Phys. Chem. A* **1998**, *102*, 2253. (b) Volkov, A. N.; Timoshkin, A. Y.; Suvorov, A. V. *Int. J. Quant. Chem*. **2004**, *100*, 412. (c) Volkov, A. N.; Timoshkin, A. Y.; Suvorov, A. V. *Int. J. Quant. Chem*. **2005**, *104*, 256. (d) Yamabe, S.; Yamazaki, S. *J. Phys. Org. Chem*. **2009**, *22*, 1094.

(19) Soriano, E.; Marco-Contelles J. *Organometallics* **2006**, *25*, 4542.

(20) Computations on the gold(I)-phosphine catalyzed hydroamination of alkynes suggest that the protodemetallation step is best achieved through a carbonyl relay, see: Kovács, G.; Ujaque, G.; Lledós, A. *J. Am. Chem. Soc*. **2008**, *130*, 853.

(21) The use of additives (such as phthalimide or pyridine *N*-oxide) that have high hydrogen-bond basicity accelerates the protodemetallation step in gold catalysis by proton shuttling, see: Wang, W.; Kumar, G. B.; Xu, B. *Org. Lett*. **2014**, *16*, 636.

(22) For computed σ-alkane $AlCl_3$ complexes: Shilina, M. I.; Smirnov, V. V.; Bakharev, R. V. *Russ. Chem. Bull. Int. Ed.* **2009**, *58*, 675.

(23) Koleva, G.; Galabov, B.; Kong, J.; Schaefer III, H. F.; Schleyer, P. v. R. *J. Am. Chem. Soc*. **2011**, *133*, 19094.

(24) Galabov, B.; Koleva, G.; Kong, J.; Schaefer III, H. F.; Schleyer, P. v. R. *Eur. J. Org. Chem*. **2014**, 6918.

(25) This value is much lower than that found with *gem*-CO_2Me in the tether (17.7 kcal/mol). This is an effect of the solvation. Without solvent correction, these values are very close: 33.9 and 34.4 respectively.

(26) Mamane, V.; Hannen, P.; Fürstner, A. *Chem. Eur. J*. **2004**, *10*, 4556.

(27) (a) Balcells, D.; Clot, E.; Eisenstein, O. Chem. Rev. **2010**, *110*, 749. (b) Rousseaux, S.; Gorelsky, S. I.; Chung, B. K. W.; Fagnou, K. *J. Am. Chem. Soc.* **2010**, *132*, 10692.

(28) Gaussian 09, Revision D.01, Frisch, M. J.; Trucks, G. W.; Schlegel, H. B.; Scuseria, G. E.; Robb, M. A.; Cheeseman, J. R.; Scalmani, G.; Barone, V.; Mennucci, B.; Petersson, G. A.; Nakatsuji, H.; Caricato, M.; Li, X.; Hratchian, H. P.; Izmaylov, A. F.; Bloino, J.; Zheng, G.; Sonnenberg, J. L.; Hada, M.; Ehara, M.; Toyota, K.; Fukuda, R.; Hasegawa, J.; Ishida, M.; Nakajima, T.; Honda, Y.; Kitao, O.; Nakai, H.; Vreven, T.; Montgomery, J. A., Jr.; Peralta, J. E.; Ogliaro, F.; Bearpark, M.; Heyd, J. J.; Brothers, E.; Kudin, K. N.; Staroverov, V. N.; Kobayashi, R.; Normand, J.; Raghavachari, K.; Rendell, A.; Burant, J. C.; Iyengar, S. S.; Tomasi, J.; Cossi, M.; Rega, N.; Millam, J. M.; Klene, M.; Knox, J. E.; Cross, J. B.; Bakken, V.; Adamo, C.; Jaramillo, J.; Gomperts, R.; Stratmann, R. E.; Yazyev, O.;

Austin, A. J.; Cammi, R.; Pomelli, C.; Ochterski, J. W.; Martin, R. L.; Morokuma, K.; Zakrzewski, V. G.; Voth, G. A.; Salvador, P.; Dannenberg, J. J.; Dapprich, S.; Daniels, A. D.; Farkas, Ö.; Foresman, J. B.; Ortiz, J. V.; Cioslowski, J.; Fox, D. J. Gaussian, Inc., Wallingford CT, 2009.

(29) Zhao, Y.; Truhlar, D. G. The M06 Suite of Density Functionals for Main Group Thermochemistry, Thermochemical Kinetics, Noncovalent Interactions, Excited States, and Transition Elements. *Theor. Chem. Acc*. **2008**, *120*, 215-241.

(30) (a) Hariharan P. C.; Pople, J. A. *Theoret. Chimica Acta* **1973**, *28*, 213. (b) Francl, M. M.; Petro, W. J.; Hehre, W. J.; Binkley, J. S.; Gordon, M. S.; DeFrees, D. J.; Pople, J. A. *J. Chem. Phys.* **1982**, *77*, 3654. (c) Rassolov, V.; Pople, J. A.; Ratner M.; Windus, T. L. *J. Chem. Phys*. **1998**, *109*, 1223.

(31) (a) Hay, P. J.; Wadt, W. R. *J. Chem. Phys*. **1985**, *82*, 270. (b) Hay, P. J.; Wadt, W. R. *J. Chem. Phys*. **1985**, *82*, 284. (c) Hay, P. J.; Wadt, W. R. *J. Chem. Phys*. **1985**, *82*, 299.

(32) (a) Barone V.; Cossi, M. *J. Phys. Chem. A*, **1998**, *102*, 1995. (b) Cossi, M.; Rega, N.; Scalmani, G.; Barone, V. *J. Comp. Chem.* **2003**, *24*, 669.

(33) (a) Lee, C.; Yang, W.; Parr, R. *Phys. Rev. B* **1988**, *37*, 785. (b) Becke, A. J. *Chem. Phys*. **1993**, *98*, 5648.

(34) Bergner, A.; Dolg, M.; Kuechle, W.; Stoll, H.; Preuss, H. *Mol. Phys*. **1993**, *80*, 1431.

(35) Marion, N.; Escudero-Adán, E. C.; Benet-Buchholz, J.; Stevens, E. D.; Fensterbank, L.; Malacria, M.; Nolan, S. P. *Organometallics* **2007**, *26*, 3256.

(36) Baker, R. J.; Davies, A. J.; Jones, C.; Kloth, M. *J. Organomet. Chem.*, **2002**, *656*, 203.